Original Article

Is dynamic contrast enhancement still necessary in multiparametric magnetic resonance for diagnosis of prostate cancer: a systematic review and meta-analysis

Zhen Liang[1], Rui Hu[1], Yongjiao Yang[2], Neng An[2], Xiaoxin Duo[3], Zheng Liu[4], Shangheng Shi[5], Xiaoqiang Liu[1]

[1]Department of Urology, Tianjin Medical University General Hospital, Tianjin 300000, China; [2]Department of Urology, Tianjin Medical University Second Hospital, Tianjin 300000, China; [3]Department of Cardiology, The Second Hospital of Hebei Medical University, Shijiazhuang 050000, China; [4]Department of Rheumatology and Immunology, Tianjin Medical University General Hospital, Tianjin 300000, China; [5]Department of Transplantation, Affiliated Hospital of Medical College Qingdao University, Qingdao 266000, China

Contributions: (I) Conception and design: Z Liang, Y Yang, X Duo, Z Liu; (II) Administrative support: Z Liu; (III) Provision of study materials or patients: R Hu, X Duo, X Liu; (IV) Collection and assembly of data: R Hu, Z Liu, Z Liang; (V) Data analysis and interpretation: R Hu, N An; (VI) Manuscript writing: All authors; (VII) Final approval of manuscript: All authors.

Correspondence to: Prof. Xiaoqiang Liu, MD, PhD. Department of Urology, Tianjin Medical University General Hospital, Tianjin 300000, China. Email: 15233367861@163.com.

Background: The purpose of this study is to systematically review the literatures assessing the value of dynamic contrast enhancement (DCE) in the multiparametric magnetic resonance imaging (mpMRI) for the diagnosis of prostate cancer (PCa).

Methods: We searched Embase, PubMed and Web of science until January 2019 to extract articles exploring the possibilities whether the pre-biopsy biparametric magnetic resonance imaging (bpMRI) can replace the position of mpMRI in the diagnosis of PCa. The sensitivity and specificity of bpMRI were all included. The study quality was assessed by QUADAS-2. Bivariate random effects meta-analyses and a hierarchical summary receiver operating characteristic plot were performed for further study through Revman 5 and Stata12.

Results: After searching, we acquired 752 articles among which 45 studies with 5,217 participants were eligible for inclusion. The positive likelihood ratio for the detection of PCa was 2.40 (95% CI: 1.50–3.80) and the negative likelihood ratio was 0.31 (95% CI: 0.18–0.53). The sensitivity and specificity were 0.77 (95% CI: 0.73–0.81) and 0.81 (95% CI: 0.76–0.85) respectively. Based on our result, pooled specificity demonstrated little difference between bpMRI and mpMRI [bpMRI, 0.81 (95% CI, 0.76–0.85); mpMRI, 0.82 (95% CI, 0.72–0.88); P=0.169]. The sensitivity, however, indicated a significant difference between these two groups [bpMRI, 0.77 (95% CI, 0.73–0.81); mpMRI, 0.84 (95% CI, 0.78–0.89); P=0.001].

Conclusions: bpMRI with high b-value is a sensitive tool for diagnosing PCa. Consistent results were found in multiple subgroup analysis.

Keywords: Prostate cancer (PCa); biparametric; multiparametric; magnetic resonance imaging (MRI); contrast media; gadolinium; meta-analysis

Submitted Sep 28, 2019. Accepted for publication Jan 15, 2020.
doi: 10.21037/tau.2020.02.03
View this article at: http://dx.doi.org/10.21037/tau.2020.02.03

Introduction

Prostate cancer (PCa) is the most commonly diagnosed disease in male around the world and its incidence and mortality have been increasing (1,2). In last several years, multiparametric magnetic resonance imaging (mpMRI) has emerged as a valuable tool for several aspects of PCa management, including detection, staging, and treatment (3,4). In order to standardize and diminish the variation in acquisition, interpretation, and reporting of prostate mpMRI, the European Society of Urogenital Radiology proposed the Prostate Imaging Reporting and Data System (PI-RADS) in 2012 (5). In December 2014, the updated and simplified PI-RADS version 2 (PI-RADSv2) was introduced to address the limitations and issues derived from the old version (3). It summarized the level of suspicion of PCa in a five-point scale based on mpMRI findings considering the combination of T2-weighted (T2W), diffusion-weighted imaging (DWI), and dynamic contrast-enhanced MRI [dynamic contrast enhancement (DCE)] (5). It is notable, however, in PI-RADSv2, DCE-MRI is considered to play only a minor role in the detection of prostate tumors, and has a secondary role to T2W and DW MRI. Recent studies have demonstrated good accuracy of biparametric-MRI (bpMRI)—the combination of T2-weighted imaging and DWI, used for tumor detection when evaluated with PSA (6-8).

DCE-MRI serves to show the perfusion parameters of tissues. It gathers information about the vascularity of tissues by assessing the signal intensity of overtime after administration of gadolinium contrast material. Greer *et al.* (9) indicated that DCE-MRI added extra benefits to the application of PI-RADSv2 because abnormal DCE-MRI findings increased the cancer detection rate in every PI-RADSv2 categories 2, 3, 4, and 5. Puech *et al.* (10) considered DCE as one of the cornerstones of mpMRI for its improvement in detection and evaluation of PCa aggressiveness. On the other hand, those who advocated the nonuse of DCE suggested that bpMRI has several advantages over mpMRI, such as shorter examination time, lower risk of allergy associated with gadolinium-based contrast agents (7,11). Aydin *et al.* (12) indicated both highly vascularized BPH nodules and prostatitis can lead to increased vessel enhancement, which may cause low specificity of mpMRI. Although the updated version of PI-RADS maps out guidelines of the interpretation of DCE-MRI and acquisition processing for imaging, Berman *et al.* (13) pointed out there were still sources of variability, such as the application of 3T scanners thus it is difficult for DCE-MRI to reproduce results across centers. In our current study, based on quantitative data, a comparison has been drawn between bpMRI and mpMRI through systematic review and meta-analysis.

Methods

Literature search

The protocol for systematic review was written according to the Cochrane Handbook for Systematic Review of Interventions version 5.1.0 (14). We searched PubMed, Embase, Web of Science to make a head to head comparison between bpMRI and mpMRI in the diagnosis of PCa, and our search strategy was as follows: (prostate cancer OR prostatic cancer OR prostate neoplasm OR prostatic neoplasm OR prostate tumor OR prostatic tumor OR prostate carcinoma OR prostatic carcinoma OR PCa) AND (magnetic resonance imaging OR MRI OR MR) AND (biparametric OR bp OR T2-weighted image and DWI OR T2-weighted imaging and DWI) until January 2019. Hand-searching of the reference lists of included studies was also performed to identify other relevant articles.

Study selection

The original studies can only be included in our network meta-analysis by meeting all the following requirements: (I) the study is published in English; (II) the available data is sufficient enough to calculate the diagnostic sensitivity and specificity of bpMRI; (III) the pathology results were provided by prostatectomy or prostate biopsy; (IV) the reported data is adequate for constructing 2×2 contingency tables with at least 10 patients. Narrative reviews, observational studies, editorials, letters comments, opinion pieces and methodological reports were all excluded. The relevant articles were selected by two researchers independently and disagreements were resolved by discussion.

Methodological quality of the included studies was evaluated by two authors independently using the same criteria as described in the Cochrane Manual for Systematic Intervention Reviews 5.2 to guarantee the quality of studies. Each item was scored as either low, high or unclear risk of bias.

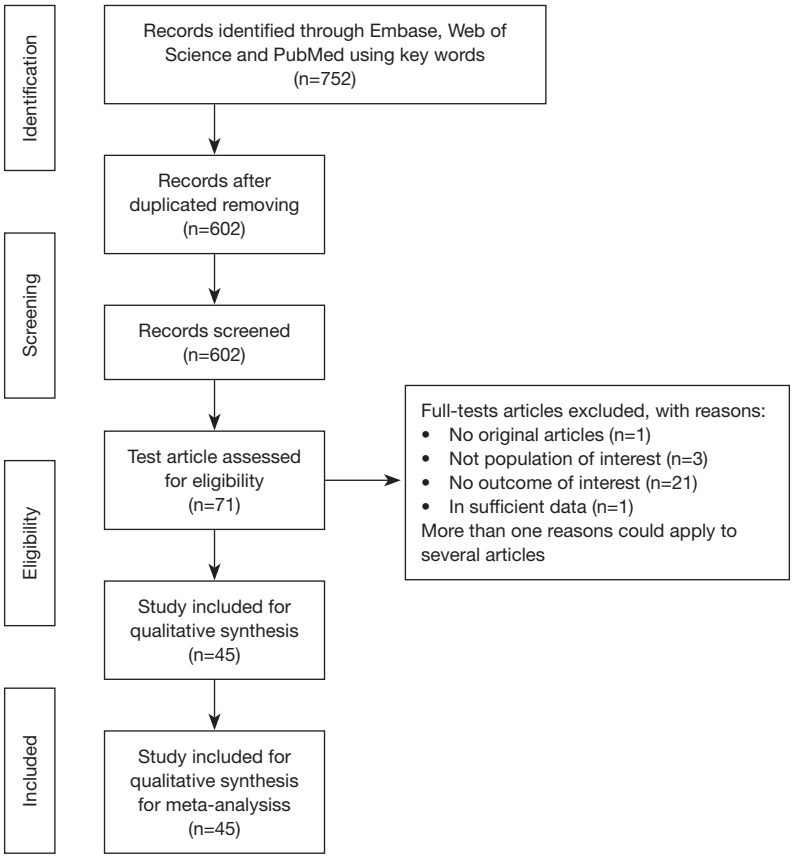

Figure 1 Flowchart summarizes selection process toward final group of studies analyzed.

Statistical analysis

Collection of results data for the quantitative synthesis was processed through Open Meta-analyst (15). All statistical analyses were conducted with the Midas module in Stata 13.1 (Stata Corporation, College Station, TX, USA). The sensitivity rate TP/(TP + FN) ×100% and specificity rate TN/(TN + FP)×100% were calculated and two forest plots were generated side by side: one for specificity and the other for sensitivity. A bivariate random effects regression was performed to calculate several primary outcomes, including diagnostic likelihood ratio positive (DLR+), diagnostic likelihood ratio negative (DLR–), and diagnostic OR (DOR) pooled sensitivity, specificity, with corresponding 95% CIs (16). The summary receiver operating characteristic curve (SROC) was used to evaluate the predictive value of each scoring system. Deek's funnel plot was conducted to detect publication bias, with $P<0.05$ suggesting publication bias. Heterogeneity was valued with the Higgins-Thompson I^2 method and the Chi-square. The significant heterogeneity was indicated by P value <0.05 and $I^2>50\%$ (17). Subgroup analysis was accomplished if there was significant heterogeneity.

Results

Study selection

The electronic databases search yielded 752 titles and abstracts, among which 602 studies were selected to be fully reviewed; after excluding 362 duplicates and 240 conference abstracts, reviews, case reports and letters to journal editors, 71 studies were assessed for eligibility. The details of study selection are demonstrated in *Figure 1*. A total of 45 studies were included in the final analysis.

The sample size ranged from 20 to 1,063, with a total of 5,217 patients included in our study. The involved 45 cohorts were carried out in the United States, Egypt, Switzerland, Germany, Denmark, France, Korea, Canada. Belgium, Japan, Finland, Austria, United States, Brazil,

Italy, Spain and Turkey respectively. Among them 15 were (8,18-31) prospective studies and 30 were retrospective studies. The publication period of these studies was from 2005 to 2018. The characteristics of included studies are presented in *Tables 1,2*. The age range of men was from 41 to 87 years (average 65.8). Across all studies, the PSA value ranged from 0.1–935.5 ng/mL. The definition of clinically significant prostate cancer (csPCa) is also varied considerably.

A total of 22 (8,18-20,27,29,31,32,35,37-39,42-44,48-50, 55-58) studies were performed on biopsy-naive patients, and 4 (7,24,32,48) studies reported on a mixed cohort (patients with previous prostate biopsy or no biopsy experience). The reference standard was based on radical prostatectomy in 23 (11,18,21-23,25,26,28,34,37-39,42,44-46,48,51,53-56,59) studies, transperineal template saturation biopsy in 3 (7,20,38) studies, targeted in-bore MRI-guided biopsy in 2 (7,33) studies, MRI-ultrasound fusion guided biopsy in 5 (32,35,41,43,47) studies. Patients of 24 (18,21-26,28,30,31,33,36,37,39,41,42,45,48,50,51,55,57-59) included studies underwent MRI with a 1.5T scanner, and 19 (7,8,11,19,20,27,29,34,38,40,41,43,46,47,49,52-54,56) studies applied 3.0T scanner. Twenty-three (8,11,19-25,27-29,31,33,36-38,41,42,44,47,50,57) studies used endorectal coil. High b values (≥1,400 s/mm^2) were applied in 11 (7,8,30,38,41,43,46,49,52-54) studies and low b values (<1,400 s/mm^2) in 34 studies. Per-patient analysis was performed in 12 (7,8,32,35,37,38,48-52,56) studies, and per-lesion analysis in 33 studies.

Assessment of study quality and publication bias

The Quality Assessment of Diagnostic Accuracy Studies tool (QUADAS) was conducted to evaluate the quality of the study. The risk of bias for, index test, patient selection, flow and timing, reference standard, as well as the concerns for applicability were displayed in *Figure 2*. As for patient selection, 14 (8,25,26,31,32,34,42-44,46,49,50,52,55) studies had high risk of bias as consecutive enrollment was not applied or mentioned in their articles. Regarding the index test domain, 7 (18,21-23,42,49,55) studies had high risk of bias because instead of prespecifying the cutoff value for diagnosing the presence of PCa, they established the values based on ROC curve analysis. Thirteen (18,19,24, 27,29,31,32,35,38,47,51,56,59) studies did not provide enough proof that whether the MRI screening results were interpreted by assessors blinded to the biopsy results. In case of reference standard, radical prostatectomy or MRI-TRUS fusion-guided targeted biopsy were considered as the low risk reference standard. Other methods such as TRUS-guided biopsy or transperineal biopsy were considered to be of high risk. Therefore, the risk of bias in the reference standard was high in 12 (8,19,20,29-31,36,40,49,50,57,58) studies. About flow and timing, 8 (7,18,26,28,38,46,55,56) studies had high risk of bias because all included patients did not undergo the same reference standard, some underwent radical prostatectomy while others underwent TRUS- or MRI-guided biopsy. Twelve (8,19,20,29-31, 36,40,49,50,57,58) studies had unclear bias for the interval between the reference standard and MRI was not provided. For applicability, 4 (18,33,36,50) studies have high risk of bias since T2W or DWI sequence was used solely instead of combining them together.

Little publication bias was detected by Begg rank correlation (with continuity correction) and Egger's linear regression test of funnel plot asymmetry in this meta-analysis with a p value of 0.55 for the slope coefficient (*Figure 3*).

Overall diagnostic accuracy

The result of the including researches was listed in *Figure 4*. The sensitivity of bpMRI for distinguishing cancerous and noncancerous specimen ranged from 45% to 99%, and the specificity ranged from 37% to 100%. The pooled sensitivity was 0.77 (95% CI: 0.73–0.81) with heterogeneity (I^2=93.55, P=0.00) and a pooled specificity of 0.81 (95% CI: 0.76–0.85) with heterogeneity (I^2=95.73, P=0.00). On the other hand, the sensitivity of bpMRI for distinguishing csPCa and insignificant PCa (insPCa) specimen ranged from 49% to 96%, and its specificity was ranged from 34% to 88%. The pooled sensitivity was 0.78 (95% CI: 0.66–0.87) with heterogeneity (I^2=96.14, P=0.00) and a pooled specificity of 0.77 (95% CI: 0.66–0.85) with heterogeneity I^2=98.00, P=0.00) (*Figure 5*). The performance of bpMRI for carcinoma in different locations was also evaluated in our present study. Concerning the peripheral zone the sensitivity of bpMRI was 75% (95% CI: 0.67–0.82) ranging from 32–91% with heterogeneity (I^2=88.64, P=0.00), and the specificity was 81% (95% CI: 0.73–0.87) ranging from 45–98% with heterogeneity (I^2=92.76, P=0.00) (*Figure 6*). The sensitivity of bpMRI for transition zone was 80% (95% CI: 0.73–0.85) ranging from 72–100% with heterogeneity (I^2=70.13, P=0.00), the specificity was 80% (95% CI: 0.70–0.87) ranging from 50–91% with heterogeneity (I^2=92.95, P=0.00) (*Figure 7*). The summary AUC was 0.86

Table 1 Basic characteristic of included studies

Author	Period	Patient number	No. of Patients with PCa	Pre-or post-biopsy MRI	MRI-reference standard interval	Mean/ median age (years)	Age range (ng/mL)	Mean/ median PSA	PSA range	Mean/ median prostate volume (cm)	Prostate volume range	Repeat setting	Definition of clinically significant cancer	Gleason score
Afifi *et al.* (18)	2016	61	54	NR	NR	NR	NR	NR	>4	NR	BR	FB	–	NR
Agha *et al.* (19)	2014	20	15	Post	NR	NR	NR	NR	NR	NR	NR	FB	–	NR
Rais-Bahrami *et al.* (32)	2015	143	84	Pre	NR	60.7	41–80	6.8	0.1–51.1	48.1	NR	FB	–	NR
Barth *et al.* (20)	2017	63	38	Pre	1–161 days	65.2	51.2–78.2	9.2	0.3–32.4	NR	NR	FB	Diameter ≥10 mm or GS ≥7 (3+4)	5–9
Baur *et al.* (33)	2014	55	55	Pre (some)	1–118 days	66	54–78	10	2.9–65.2	65	49–88	FB & PNB	–	6–10
Boesen *et al.* (8)	2018	1,020	655	Pre	NR	67	61–71	8	5.7–13	NR	NR	FB	GS ≥3+4	6–10
Brock *et al.* (21)	2015	45	41	Post	NR	66	NR	66	NR	37.5	NR	NR	–	≥6
Delongchamps *et al.* (22)	2011	58	58	Post	NR	62	49–74	6.8	4–9.9	35	20–120	NR	–	NR
Delongchamps *et al.* (23)	2011	57	57	Post	NR	63	54–76	7	2.8–28	NR	NR	NR	–	≤6 to ≥7
Doo *et al.* (34)	2012	51	51	Post	>3 weeks	63	50–72	11.5	4.23–43.83	NR	NR	NR	GS ≥7	6–10
Fascelli *et al.* (35)	2016	59	44	Pre	NR	64.3	45.0–84.9	6.8	0.9–43.3	49.1	NR	FB	GS ≥7	NR
Franiel *et al.* (24)	2011	54	21	Pre	2–120 days	68	49–78	12.1	3.3–65.2	NR	NR	FB & PNB	–	6–10
Haider *et al.* (25)	2007	44	44	Post	>6 weeks	61	46–75	5.375	0.9–26	NR	NR	NR	Gs ≥6 and diameter >4 mm	6–10
Isebaert *et al.* (26)	2013	75	75	Pre	1–149 days	66	49–74	10.4	1.5–70.9	NR	NR	NR	≥5 mm	6–10
Iwazawa *et al.* (36)	2011	178	72	NR	<44 days	68.8	41–86	20.5	4.04–568.5	NR	NR	NR	–	6–9
Jambor *et al.* (27)	2015	55	37	Post	1–217 days	66	47–76	7.4	4–14	42	17–107	FB	Gs ≥3+3 and diameter >3 mm	6–9

Table 1 (*continued*)

Table 1 (*continued*)

Author	Period	Patient number	No. of Patients with PCa	Pre-or post-biopsy MRI	MRI-reference standard interval	Mean/ median age (years)	Age range (ng/mL)	Mean/ median PSA	PSA range	Mean/ median prostate volume (cm)	Prostate volume range	Repeat setting	Definition of clinically significant cancer	Gleason score
Jung *et al.* (37)	2013	156	72	Pre	0–189 days	59.2	42–79	5	0.2–78.1	NR	NR	FB	Diameter ≥5 mm	≥6
Junker *et al.* (38)	2019	236	135	Pre	NR	67.6	NR	6.4	1.89–88.44	45	15–190	FB	–	6–9
Katahira *et al.* (39)	2011	201	201	Post	RP: >2 months; biopsy: >1 month	70	43–80	8.6	2.61–114	NR	NR	FB	–	4–10
Kitajima *et al.* (40)	2010	53	30	Pre	10–41 days	69	56–84	11.1	4.2–112.1	NR	NR	NR	–	NR
Kitamura *et al.* (28)	2014	54	54	Post	24.8–54.5 days	62.7	NR	5.7	4.4–7.6	NR	NR	NR	–	≥6
Kuhl *et al.* (7)	2017	542	138	Pre	28–169 days	65	42–80	7	3.2–67.5	52	13–196	FB & PNB	PSA ≥10, GS ≥7≥ T2	6–10
Lawrence *et al.* (41)	2014	39	16	Pre	>9 months	64	47–77	10	1.2–36	NR	NR	PNB	–	6–9
Lee *et al.* (29)	2017	55	23	Pre	NR	mpMRI: 61.8; bpMRI: 62.0	NR	mpMRI: 6.7; bpMRI: 6.19	NR	mpMRI: 38.6; bpMRI: 40.2	NR	FB	–	6–10
Lim *et al.* (42)	2009	52	52	Post	2–38 days	65	48–76	10.5	1.2–79.6	NR	NR	FB	–	6–9
Morgan *et al.* (30)	2007	54	54	Post	<3 months	68	52–80	9.8	2.3–46	NR	NR	NR	–	6–9
Mussi *et al.* (43)	2017	118	68	Pre	<16 months	NR	NR	4.6	3.8–7.0	45	35–70	FB	NR	≥6
Naiki *et al.* (44)	2011	35	35	Pre	NR	67.7	49–78	12.8	2.78–67.3	NR	NR	FB	–	5–10
Rinaldi *et al.* (31)	2012	41	36	Post (some)	48±54 days	69	57–80	15.15	5.98–133	NR	NR	FB	–	NR
Rosenkrantz *et al.* (45)	2011	42	42	Post	NR	62	47–76	6.2	1.3–32.5	NR	NR	NR	–	6–9

Table 1 (*continued*)

Table 1 (*continued*)

Author	Period	Patient number	No. of Patients with PCa	Pre-or post-biopsy MRI	MRI-reference standard interval	Mean/ median age (years)	Age range (ng/mL)	Mean/ median PSA	PSA range	Mean/ median prostate volume (cm)	Prostate volume range	Repeat setting	Definition of clinically significant cancer	Gleason score
Scialpi *et al.* (46)	2017	41	41	Post	28–121 days	64.5	53–78	6.8	1.5–39.3	NR	NR	NR	GS ≥7	≥6
Schimmöller *et al.* (47)	2014	235	115	Post	4–6 weeks	65.7	NR	9.9	NR	57.9	NR	FB & PNB	–	NR
Shimofusa *et al.* (48)	2005	60	37	Post	<6 months	71	54–82	21.8	4.5–130	NR	NR	FB	–	NR
Stanzione *et al.* (49)	2016	82	34	Pre	20–30 days	65	43–84	8.8	NR	62.9	NR	FB	–	6–9
Tamada *et al.* (50)	2011	50	35	Pre	1–87 days	65	45–75	6.68	4.06–9.94	NR	NR	FB	–	6–10
Tanimoto *et al.* (51)	2007	83	44	Pre	<4 months	67.4	53–87	19.4	4.3–332.1	NR	NR	NR	–	6–10
Thestrup *et al.* (52)	2016	204	68	Post (some)	<3 months	65	45–75	14	2.2–120	60	23–263	NR	GS ≥7	NR
Ueno *et al.* (53)	2013	80	80	Post	28±33 days	66.5	50–77	9.51	2.9–49	NR	NR	NR	–	6–9
Ueno *et al.* (54)	2013	73	73	Post	NR	66	50–77	9.51	2.9–49	NR	NR	NR	–	6–9
Vargas *et al.* (11)	2011	51	51	Post	<6 months	58	46–74	5.3	0.4–62.2	NR	NR	NR	–	6–8
Vilanova *et al.* (55)	2010	70	38	Pre	13±9 days	63.5	43–87	7.4	4–17.20	NR	NR	FB	–	6–8
Visschere *et al.* (56)	2017	245	198	NR	<2 years	66	44–85	9	1.4–935.5	NR	NR	FB	GS ≥7c, ≥0.5 mL, or extraprostatic extension	NR
Yağci *et al.* (57)	2011	43	21	Pre	NR	66	49–79	9.4	1.4–120	NR	NR	FB	–	6–10
Yoshimitsu *et al.* (58)	2008	37	37	Post	6–9 weeks	66	56–75	11.9	0.7–54.8	49.3	19.8–201	FB	–	NR
Yoshizako *et al.* (59)	2009	23	23	Post	1–7 weeks	68	52–81	NR	NR	NR	NR	NR	–	6–9

PNB, previous negative biopsy; FB, first biopsy; NR, not reported.

Table 2 Basic characteristic of included studies

Author	Study design	Consecutive enrollment	Reference Standard	Blinding	Field strength (T)	b value (s/mm^2)	Type of Analysis	Localization	Endorectal coil	ADC map
Afifi *et al.* (18)	Prospective	Y	TRUSGB and RP	NR	1.5	0, 800, 1,000	Lesion	PZ, TZ, whole	N	Y
Agha *et al.* (19)	Prospective	Y	TRUSGB	NR	3	0, 1,000	Lesion	Whole	Y	Y
Rais-Bahrami *et al.* (32)	Retrospective	NR	MRI-TRUSGB	NR	NR	NR	Patient	Whole	NR	NR
Barth *et al.* (20)	Prospective	N	TTSB	Y	3	0,50, 1,000 or 100, 600, 1,000	Lesion	Whole	Y	NR
Baur *et al.* (33)	Retrospective	Y	Targeted MRGB	Y	1.5	0, 100, 400, 800	Lesion	PZ, TZ, whole	Y	Y
Boesen *et al.* (8)	Prospective	NR	TRUSGB	Y	3	0, 100, 800, and 2,000	Patient	Whole	Y	NR
Brock *et al.* (21)	Prospective	Y	RP	Y	1.5	NR	Lesion	Whole	Y	NR
Delongchamps *et al.* (22)	Prospective	Y	RP	Y	1.5	0, 800	Lesion	PZ, TZ, whole	Y	Y
Delongchamps *et al.* (23)	Prospective	Y	RP	Y	1.5	0, 800	Lesion	PZ, TZ, whole	Y	Y
Doo *et al.* (34)	Retrospective	NR	RP	Y	3	0, 1,000	Lesion	Whole	N	Y
Fascelli *et al.* (35)	Retrospective	Y	MRI-TRUSGB	NR	NR	NR	Patient	Whole	NR	Y
Franiel *et al.* (24)	Prospective	Y	TRUSGB and MRGB	NR	1.5	0, 100, 400, 800	Lesion	Whole	Y	Y
Haider *et al.* (25)	Prospective	NR	RP	Y	1.5	600	Lesion	PZ, TZ, Whole	Y	Y
Isebaert *et al.* (26)	Prospective	NR	TRUSGB and RP	Y	1.5	NR	Lesion	Whole	N	Y
Iwazawa *et al.* (36)	Retrospective	Y	TRUSGB	Y	1.5	0, 1,000	Lesion	PZ, TZ, whole	Y	Y
Jambor *et al.* (27)	Prospective	Y	TRUSGB and MRGB	NR	3	0, 100, 200, 350	Lesion	Whole	Y	Y
Jung *et al.* (37)	Retrospective	Y	RP	Y	1.5	0, 1,000	Patient	TZ	Y	Y
Junker *et al.* (38)	Retrospective	Y	TTSB and RP	NR	3	50, 400, 1,000 s/mm^2 before 2014 and 50, 500, 1,400 s/mm^2 after 2014	Patient	Whole	Y	NR
Katahira *et al.* (39)	Retrospective	Y	RP	Y	1.5	500	Lesion	PZ, TZ, Whole	N	Y
Kitajima *et al.* (40)	Retrospective	Y	TRUSGB	Y	3	0, 1,000	Lesion	PZ, TZ, Whole	N	Y
Kitamura *et al.* (28)	Prospective	Y	TRUSGB and RP	Y	1.5	NR	Lesion	Whole	Y	Y

Table 2 (*continued*)

Table 2 (*continued*)

Author	Study design	Consecutive enrollment	Reference Standard	Blinding	Field strength (T)	b value (s/mm^2)	Type of Analysis	Localization	Endorectal coil	ADC map
Kuhl *et al.* (7)	Retrospective	Y	TRUSGB and RP and TTSB and Targeted MRGB	Y	3	0, 800, 1,000, 1,400	Patient	Whole	N	NR
Lawrence *et al.* (41)	Retrospective	Y	MRI-TRUSGB	Y	1.5 or 3	0, 1,000, 1,400	Lesion	PZ, TZ	Y	Y
Lee *et al.* (29)	Prospective	Y	TRUSGB	NR	3	0, 1,000	Lesion	Whole	Y	Y
Lim *et al.* (42)	Retrospective	NR	RP	Y	1.5	0, 1,000	Lesion	Whole	Y	Y
Morgan *et al.* (30)	Prospective	Y	TRUSGB	Y	1.5	50, 400, 800, 1,500	Lesion	Whole	N	Y
Mussi *et al.* (43)	Retrospective	NR	MRI-TRUSGB	Y	3	50, 400, 800, 1,500	Lesion	Whole	N	Y
Naiki *et al.* (44)	Retrospective	NR	TRUSGB and RP	Y	NR	0, 800	Lesion	PZ, TZ, whole	Y	Y
Rinaldi *et al.* (31)	Prospective	NR	TRUSGB	NR	1.5	0, 250, 500, 750, 1,000	Lesion	PZ, CZ, whole	Y	Y
Rosenkrantz *et al.* (45)	Retrospective	Y	RP	Y	1.5	0, 500, 1,000	Lesion	PZ	N	Y
Scialpi *et al.* (46)	Retrospective	NR	TRUSGB and RP	Y	3	0, 2,000	Lesion	PZ, TZ, whole	N	Y
Schimmöller *et al.* (47)	Retrospective	Y	MRI-TRUSGB	NR	3	0, 250, 500, 750, 1,000	Lesion	PZ, TZ, whole	Y	Y
Shimofusa *et al.* (48)	Retrospective	Y	RP	Y	1.5	0, 1,000	Patient	Whole	N	NR
Stanzione *et al.* (49)	Retrospective	NR	TRUSGB	Y	3	0, 400, 2,000	Patient	Whole	N	Y
Tamada *et al.* (50)	Retrospective	NR	TRUSGB	Y	1.5	NR	Patient	Whole	Y	Y
Tanimoto *et al.* (51)	Retrospective	Y	RP	NR	1.5	0, 1,000	Patient	Whole	N	Y
Thestrup *et al.* (52)	Retrospective	NR	TRUSGB and MRGB	Y	3	0, 100, 800, 2,000	Patient	Whole	N	Y
Ueno *et al.* (53)	Retrospective	Y	RP	Y	3	0, 1,000, 2,000	Lesion	PZ, TZ, whole	N	Y
Ueno *et al.* (54)	Retrospective	Y	RP	Y	3	0, 1,000, 2,000	Lesion	PZ, TZ, whole	N	Y
Vargas *et al.* (11)	Retrospective	Y	RP	Y	3	0, 700, 1,000	Lesion	Whole	Y	Y
Vilanova *et al.* (55)	Retrospective	NR	TRUSGB and RP	Y	1.5	0, 1,000	Lesion	PZ	N	Y
Visschere *et al.* (56)	Retrospective	NR	TRUSGB and RP	NR	3	NR	Patient	Whole	N	Y
Yağci *et al.* (57)	Retrospective	Y	TRUSGB	Y	1.5	800	Lesion	TZ	Y	Y
Yoshimitsu *et al.* (58)	Retrospective	NR	TRUSGB	Y	1.5	0, 500, 1,000	Lesion	PZ, TZ, whole	N	Y
Yoshizako *et al.* (59)	Retrospective	NR	RP	NR	1.5	0, 1,000	Lesion	TZ	N	Y

PZ, peripheral zone; RP, radical prostatectomy; TRUSGB, transrectal ultrasound-guided standard biopsy; NR, not given; Y, yes; N, no; TZ, transitional zone.

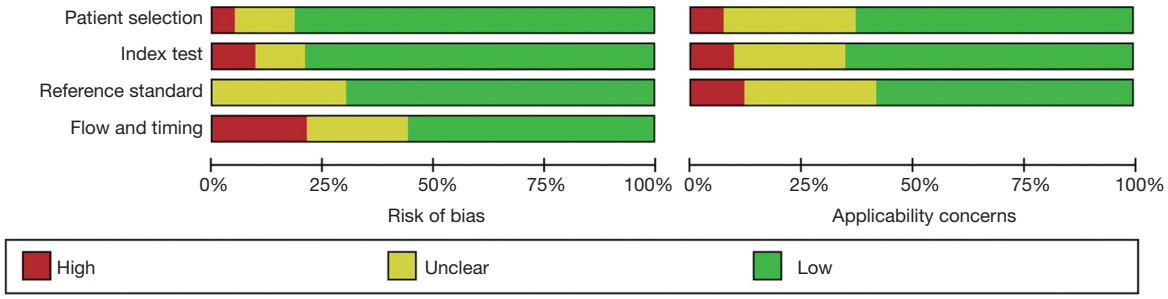

Figure 2 Chart shows summary of results of methodologic quality analysis of 45 studies in meta-analysis according to Quality Assessment of Diagnostic Accuracy Studies 2.

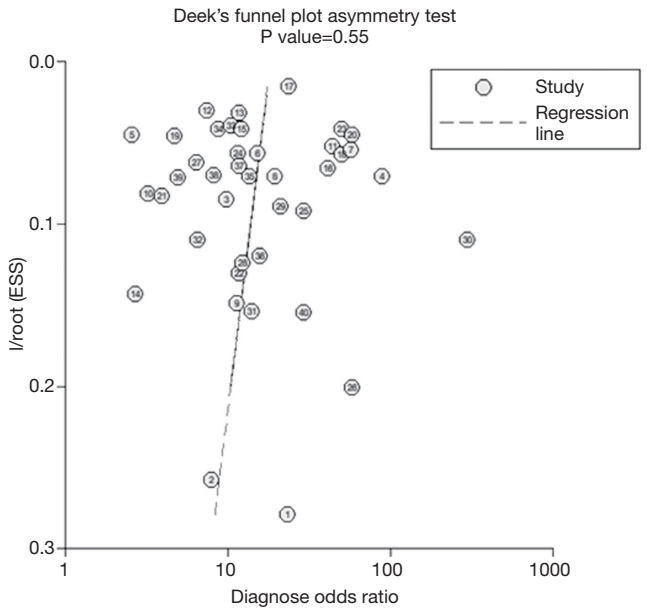

Figure 3 Plot results of Deeks funnel plot asymmetry test (P=0.55) show log odds ratios for visualization of publication bias

for overall cancer and 0.84 for csPCa which is similar to the performance of mpMRI (0.90, 0.83 for overall PCa and csPCa respectively) (*Figures 8,9*). For the cancer located at the peripheral zone, the summary AUC of bpMRI was 0.85 (*Figure 10A*), while the AUC was 0.86 for transition zone cancer (*Figure 10B*). In addition, the overall positive LR and negative LR for the overall PCa 4.10 (95% CI: 3.30–5.10) and 0.28 (95% CI: 0.24–0.33), respectively. As for csPCa, the positive LR and negative LR were 3.40 (95% CI: 2.4–4.9) and 0.29 (95% CI: 0.18–0.45) respectively, and DOR, 15 (95% CI, 11–20) for PCa, 12 (95% CI, 6–22) for csPCa. The overall positive LR and negative LR for the peripheral zone cancer were 3.90 (95% CI: 2.70–5.60) and 0.31 (95% CI: 0.23–0.40). For the transitional zone cancer, the overall positive LR and negative LR were 3.90 (95% CI: 2.60–5.80) and 0.25 (95% CI: 0.19–0.34) respectively. As for DOR, 13 (95% CI, 8–21) for peripheral zone cancer, 15 (95% CI, 9–27) for transitional zone cancer.

Subgroup analyses and head-to-head comparison

Subgroup analysis was conducted based on study design, patient enrollment, localization the coil application, magnetic strength, b values, reference standard, blind method application and unit for analysis. Results of all subgroup analysis were summarized in *Table 3*. In accordance with the above results, the distinction among included studies could be explained as a source of the heterogeneity for the diagnosis of PCa, and our result revealed that all the factors mentioned above accounted for the heterogeneity of sensitivity while none of them had an impact on specificity.

Our studies provided head-to-head comparison between bpMRI and mpMRI. As a result, the pooled specificity demonstrated little difference between bpMRI and mpMRI [bpMRI, 0.81 (95% CI, 0.76–0.85); mpMRI, 0.82 (95% CI, 0.72–0.88); P=0.169]. The sensitivity, however, indicated a significant difference between these two groups [bpMRI, 0.77 (95% CI, 0.73–0.81); mpMRI, 0.84 (95% CI, 0.78–0.89); P=0.001] (*Figures 4,11*).

Discussion

Overall, we found very considerable diagnostic accuracy and precision for detection of PCa using bpMRI. Based on our assays, pooled sensitivity of bpMRI was 7% lower than that of mpMRI with statistical difference. Although the high sensitivity means higher confidence that a negative

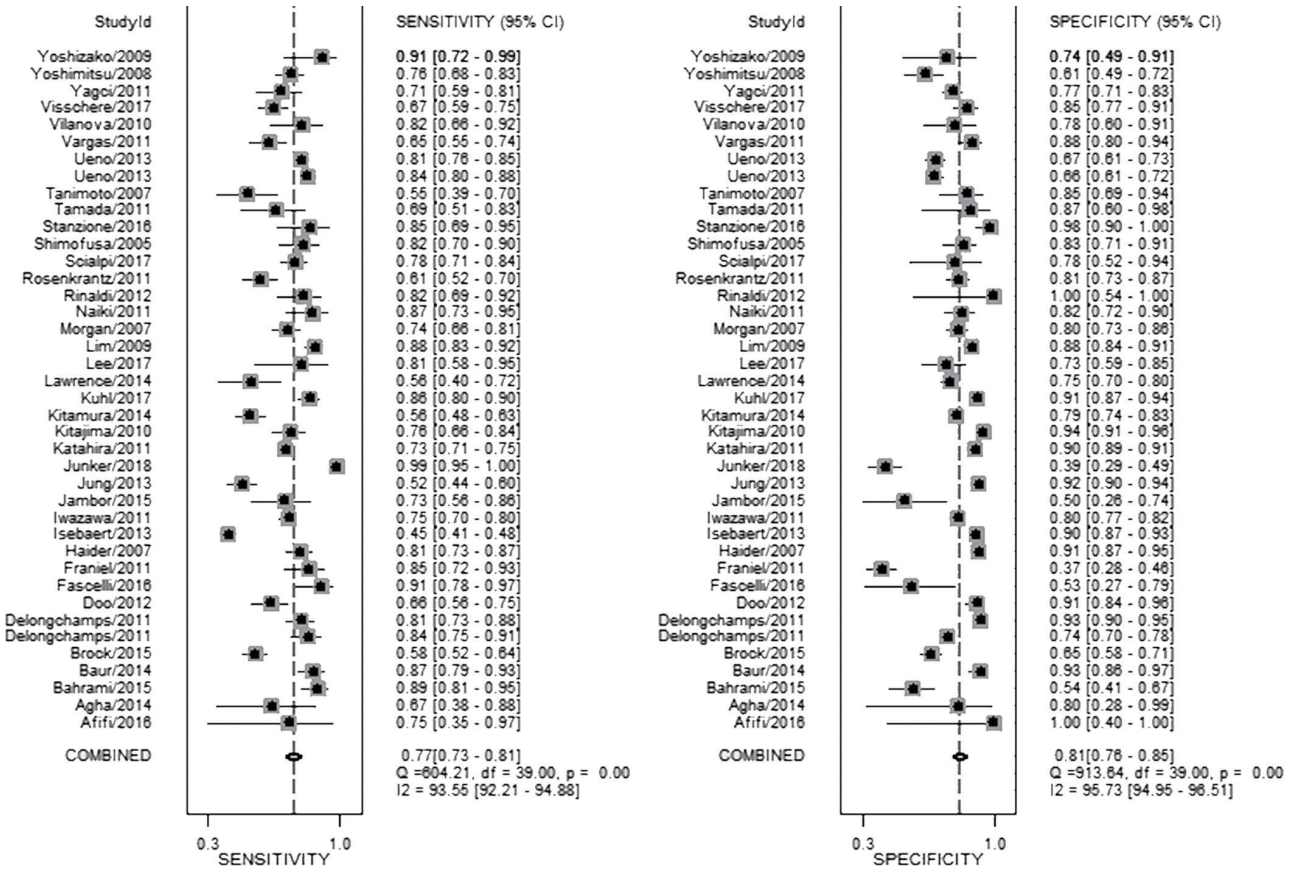

Figure 4 Coupled forest plots show pooled estimates of sensitivity and specificity of biparametric MRI for overall cancer.

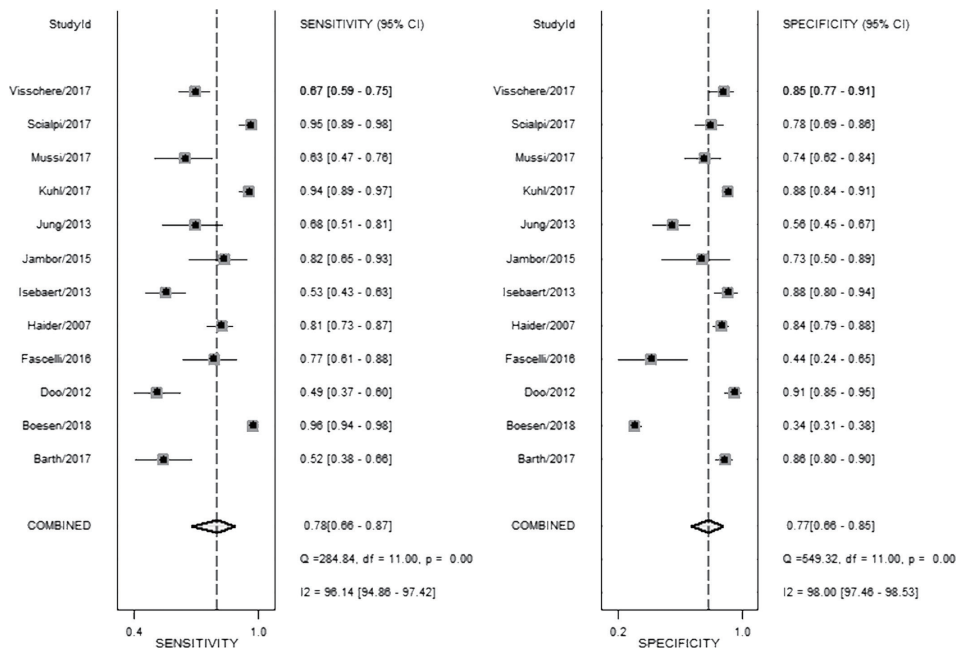

Figure 5 Coupled forest plots show pooled estimates of sensitivity and specificity of biparametric MRI for clinically significant cancer.

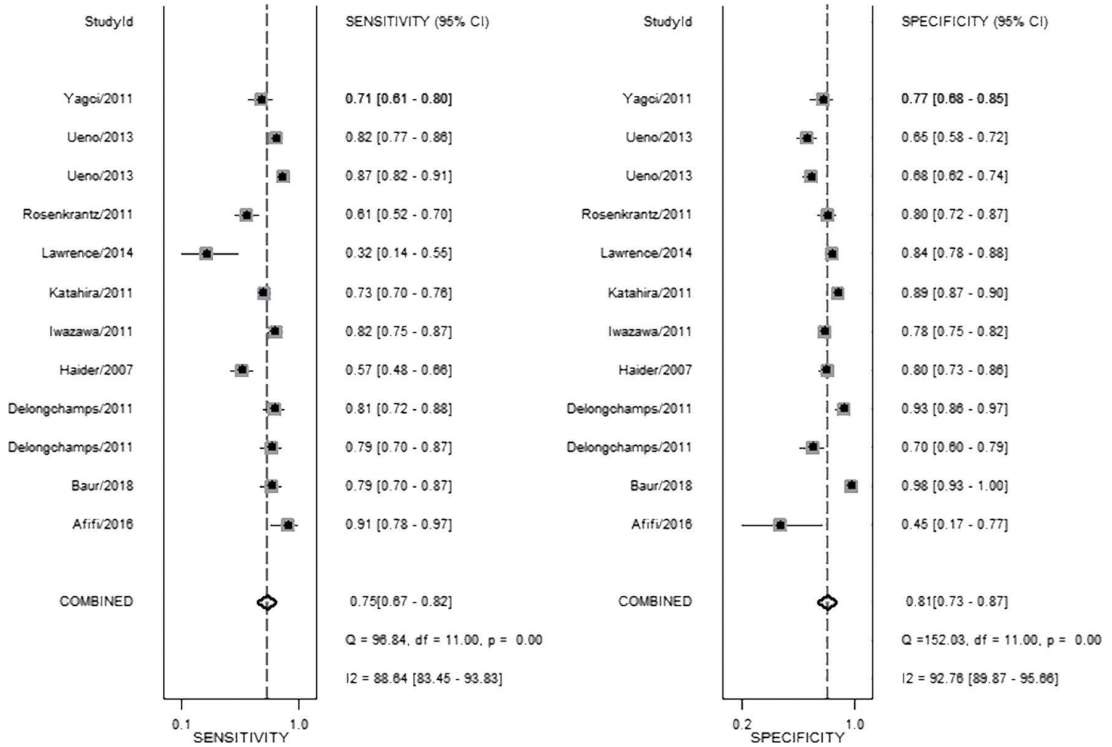

Figure 6 Coupled forest plots show pooled estimates of sensitivity and specificity of biparametric MRI for cancer located at peripheral zone.

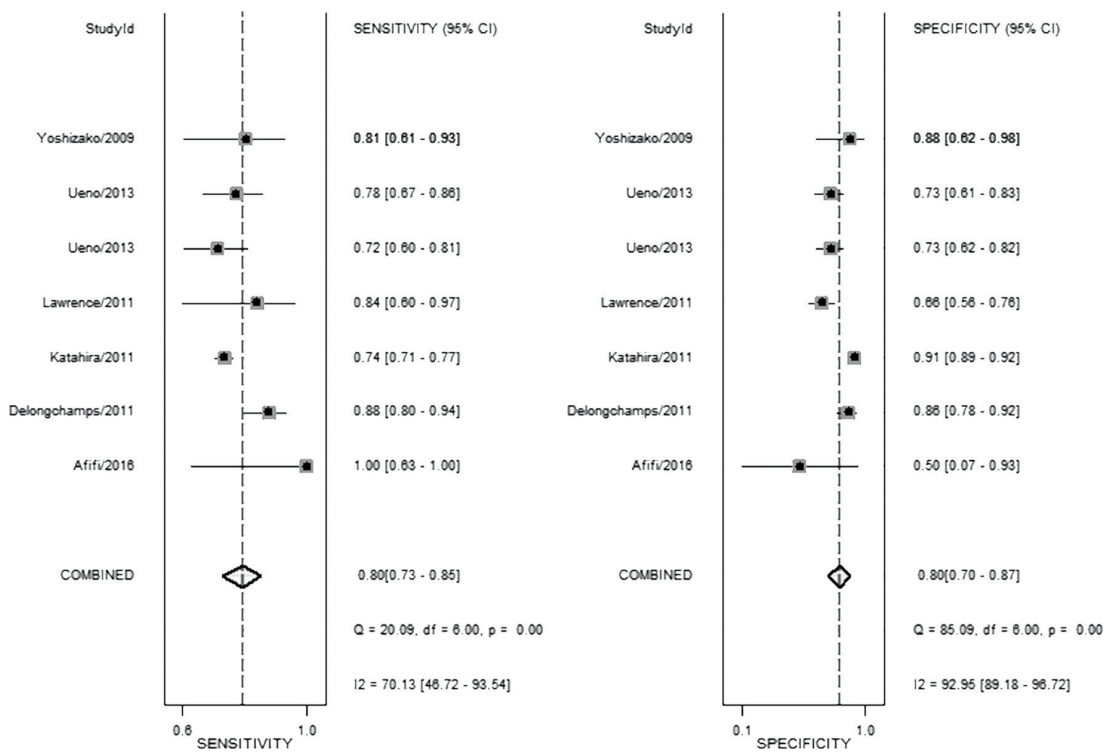

Figure 7 Coupled forest plots show pooled estimates of sensitivity and specificity of biparametric MRI for cancer located at transition zone.

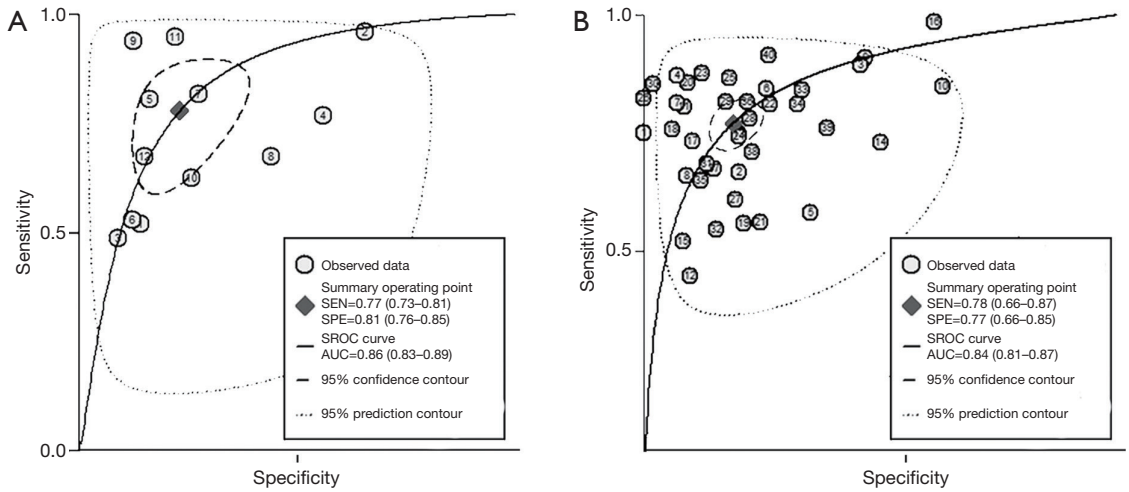

Figure 8 Summary ROC (SROC) curves with prediction and confidence contours of biparametric MRI for overall cancer (A) and clinically significant cancer (B).

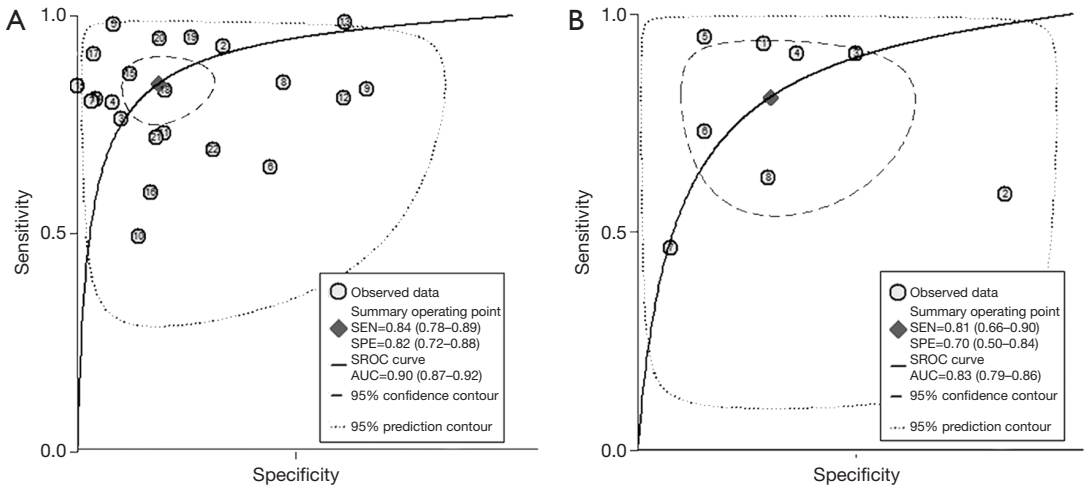

Figure 9 Summary ROC (SROC) curves with prediction and confidence contours of multiparametric MRI for overall cancer (A) and for clinically significant cancer (B).

result would be a true negative, thus reducing the likelihood of additional intervention such as prostate biopsy, the 7% lower sensitivity of bpMRI may be an acceptable trade-off for lower potential risk of adverse effects and therapy cost. Besides, the relatively low sensitivity of bpMRI could be fixed through combining with other clinical indicators. Boesen *et al.* (60) revealed positive potential for a model combining bpMRI and prostate-specific antigen density (PSAD) for detection of PCa among 808 biopsy-naïve men. Knaapila *et al.* (61) indicated PSAD could improve the NPV among men with equivocal suspicion on bpMRI, this imaging criteria coupled as an adjunct with PSA level and PSAD, could provide even more accuracy in detecting csPCa. Moreover, the issue of access to MRI caused by limited availability may be remedied through the shorter acquisition time (62). Given the impressive specificity and sensitivity of bpMRI, it may be considered as a pre-biopsy test for PCa, in place of mpMRI.

Three systematic reviews (including two meta-analyses regarding) which explored the role of mpMRI in localized PCa have been published recently. In the study by Niu *et al.* (63) which evaluated 33 studies using a combination of T2WI, DWI, the pooled sensitivity and specificity were 0.81 (95% CI: 0.76–0.85) and 0.77 (95% CI: 0.69–0.84),

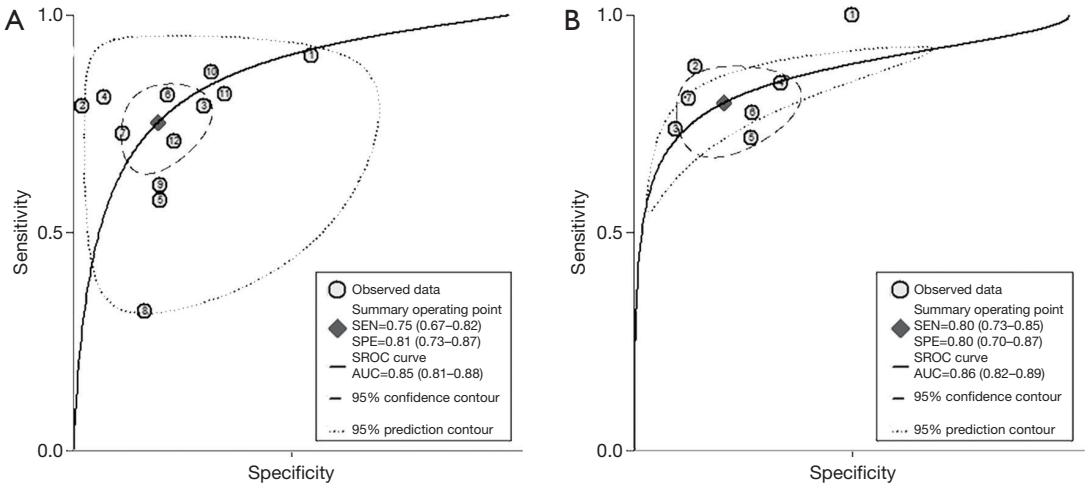

Figure 10 Summary ROC (SROC) curves with prediction and confidence contours of biparametric MRI for cancer located at peripheral zone (A) and transition zone (B).

Table 3 Subgroup analysis of analysis

Parameter	Category	Number of studies	Sensitivity	P1	Specificity	P2
Coil	Used	20	0.79 (0.73–0.84)	<0.05	0.81 (0.75–0.87)	0.69
	Not used	18	0.72 (0.66–0.79)		0.83 (0.78–0.89)	
Magnetic	3	13	0.74 (0.69–0.79)	<0.05	0.85 (0.81–0.88)	0.65
	1.5	23	0.83 (0.77–0.90)		0.66 (0.55–0.77)	
Reference	RP or targeted biopsy	24	0.77 (0.72–0.83)	<0.05	0.80 (0.75–0.86)	0.17
	Others	15	0.75 (0.68–0.82)		0.84 (0.77–0.90)	
ADC map	Used	35	0.76 (0.72–0.81)	<0.05	0.79 (0.74–0.84)	0.57
	Not used	6	0.79 (0.69–0.89)		0.89 (0.82–0.96)	
Enrollment	Consecutive	26	0.76 (0.71–0.82)	<0.05	0.79 (0.74–0.85)	0.77
	Not consecutive	14	0.78 (0.71–0.85)		0.85 (0.78–0.91)	
Blinding	Blinded	28	0.74 (0.69–0.79)	<0.05	0.85 (0.81–0.88)	0.97
	Not mention	11	0.83 (0.77–0.90)		0.66 (0.55–0.77)	
B-values	High (>1,400)	7	0.79 (0.70–0.87)	<0.05	0.82 (0.72–0.92)	0.96
	Low (≤1,400)	26	0.78 (0.73–0.83)		0.82 (0.77–0.88)	

respectively. In a more recent meta-analysis by Woo *et al.* (6) which analyzed 20 studies, the pooled sensitivity and specificity were 0.74 (95% CI: 0.66–0.81) and 0.90 (95% CI: 0.87–0.93), respectively. Compared with the former review, the current study is the first meta-analysis to evaluate the performance of bpMRI based on different location of PCa, and assess their discrimination between bpMRI and mpMRI in the detection of csPCa.

From our present study, bpMRI may be sufficient and may not miss csPCa. The pooled specificity demonstrated no significant difference between bpMRI and mpMRI [bpMRI, 0.77 (95% CI, 0.66–0.85); mpMRI, 0.70 (95% CI, 0.50–0.84); P=0.518]. The pooled sensitivity also indicated little significant difference between these two groups [bpMRI, 0.78 (95% CI, 0.66–0.87); mpMRI, 0.81 (95% CI, 0.66–0.90); P=0.135] (*Figures 5,12*). It means those tumors

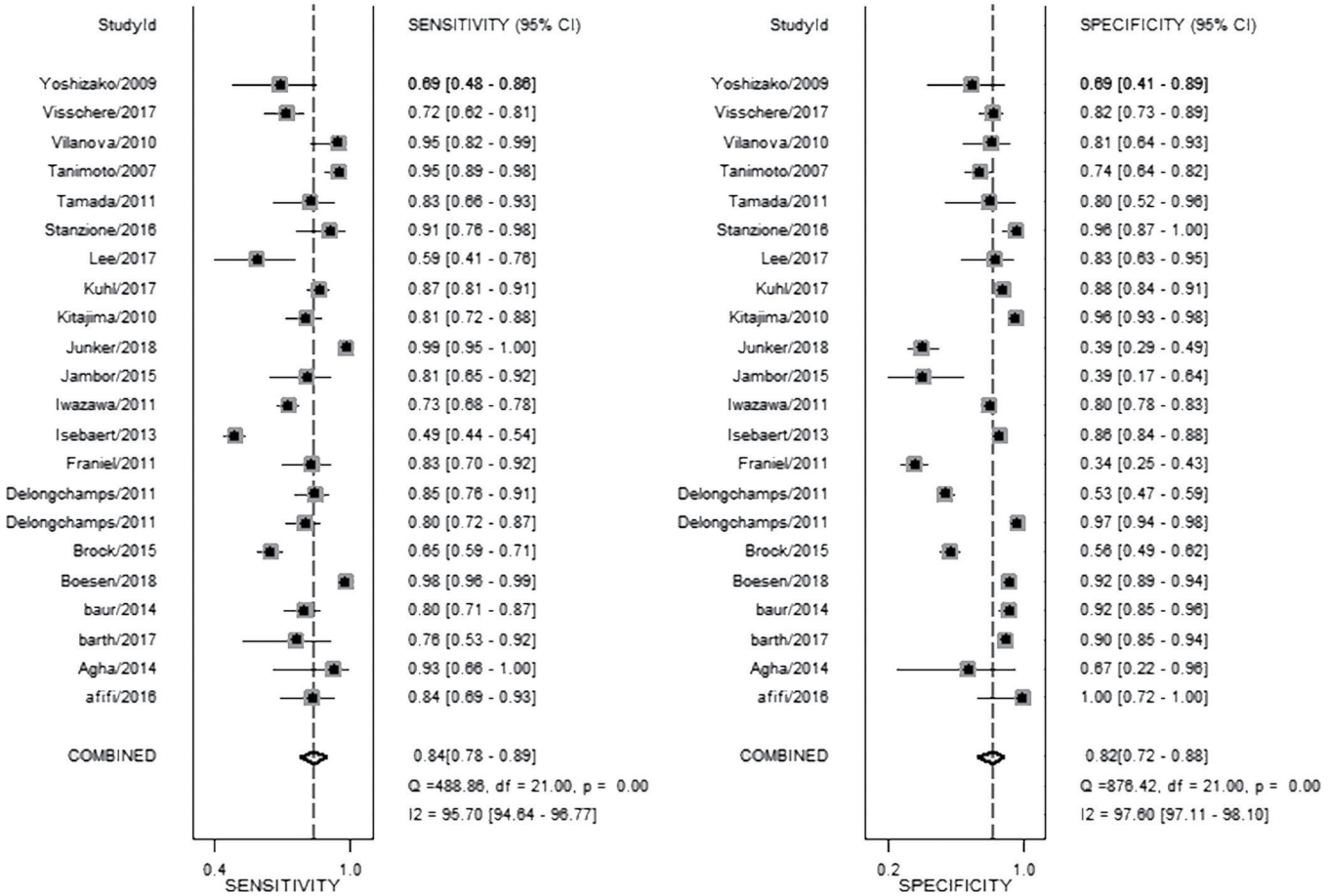

Figure 11 Coupled forest plots show pooled estimates of sensitivity and specificity of multiparametric MRI for overall cancer

ignored by bpMRI are mostly clinical insignificant and may also be ignored by mpMRI. Moreover, these tumors are more likely to remain latent in long-term follow-up and active surveillance.

Barth *et al.* (20) suggested that for the diagnose of csPCa, there is no significant difference between the diagnostic performance of a bpMRI and mpMRI protocol, which met our results. Boesen *et al.* (8) demonstrated the high NPV of bpMRI in ruling out csPCa in biopsy-naive men, a simple, rapid bpMRI method could be used as a triage test to improve risk stratification and to exclude aggressive disease and avoid unnecessary biopsies. On the other hand, Greer *et al.* (9) indicated that adding DCE-MRI to DWI scores in the peripheral zone yielded meaningful progress for detecting csPCa. Although the application of bpMRI prior to biopsy could decrease the risk of over-biopsy, reduce rates of over-detection, future work must be finished for bpMRI towards maintaining the same high diagnostic yield of mpMRI without compromising oncologic outcomes and cancer detection.

Based on our current results, for the detection of cancer located at transitional zone, both the sensitivity and specificity did not demonstrate a significant difference between these two groups [sen: bpMRI, 0.80 (95% CI, 0.73–0.85); mpMRI, 0.75 (95% CI, 0.45–0.91); P=0.0845,spe: bpMRI, 0.80 (95% CI, 0.70–0.87); mpMRI, 0.86 (95% CI, 0.74–0.93); P=0.0982] DWI alone is enough for cancer located in transitional zone which met the results of PI-RADSv2. While for the cancer located in peripheral zone, the pooled specificity demonstrated significant difference between bpMRI and mpMRI [bpMRI, 0.81 (95% CI, 0.73–0.87); mpMRI, 0.96 (95% CI, 0.92–0.98); P<0.05]. The sensitivity, however, indicated little significant difference between these two groups [bpMRI, 0.75 (95% CI, 0.67–0.82); mpMRI, 0.74 (95% CI, 0.66–0.80); P=0.943].

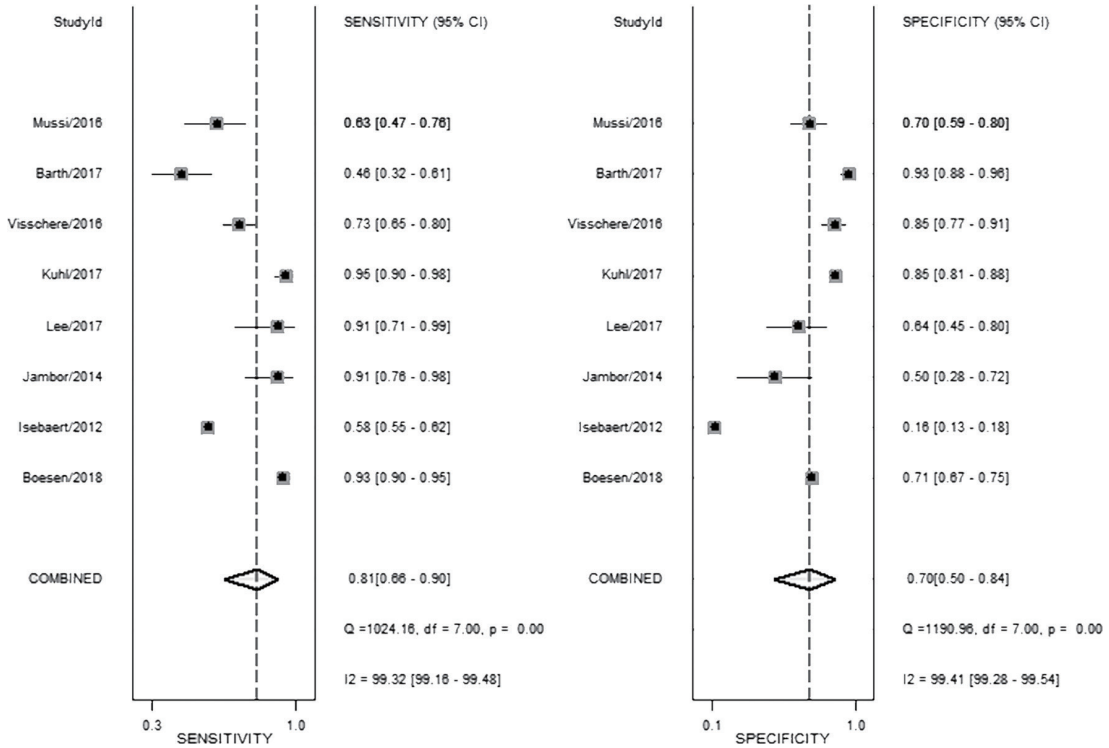

Figure 12 Coupled forest plots show pooled estimates of sensitivity and specificity of multiparametric MRI for clinically significant cancer.

From our analysis, the application of DCE contributes to unignorable improvements in specificity for peripheral PCa. Multiple studies have demonstrated that DCE-MRI can successfully detect PCa with a high sensitivity and specificity and help in tumor staging in peripheral zone (64-66). However, Delongchamps *et al*. (23) suggested DCE-MRI may decrease the accuracy of T2WI and DWI for the cancer located at the central gland without significant improvement in peripheral zone. These debatable reports might be explained by different references to evaluate DCE-MRI in a quantitative way. After the PI-RADS score was updated in 2016 by ESUR and American College of Radiology (3), the question whether DCE-MRI could lead to an added value and better performance in the interpretation of mpMRI might be answered in the future.

The b-value is one of the significant factors that lead to the heterogeneity based on our subgroup analysis, it reflects the timings and strength of magnetic field gradients of DWI applied to the patient, and the collection of multiple b-values permits the calculation of ADC map. Currently, based on the PI-RADSV2, the recommended b-values is at least 1,400 s/mm^2, or if possible, up to 2,000 s/mm^2 (3). Our subgroup analysis demonstrated that high b values ≥1,400 s/mm^2 lead to significantly higher sensitivity and specificity for detecting PCa, Therefore, forest plots were also accomplished in present study to make a comparison between mpMRI and bpMRI with high b values ≥1,400 s/mm^2 (*Figure 13*). As shown in our results, there is no significant difference in both sensitivity [bpMRI with high b values 0.83 (95% CI, 0.72–0.90); mpMRI 0.84 (95% CI, 0.78–0.89), P=0.431] and specificity [bpMRI with high b values 0.78 (95% CI, 0.63–0.88); mpMRI 0.82 (95% CI, 0.72–0.88) P=0.621] (*Figures 11,13*). The AUC is 0.88 which is similar to that of mpMRI (AUC =0.90) (*Figures 9,14*). Maas *et al.* (67) indicated that the application of high-b-value computed could avoid artefacts and improve lesion-to-background contrast ratios for the detection of PCa. Syer *et al.* (68) suggested that diagnostic accuracy of combined DWI and T2WI is trustable with high b-values improving sensitivity while maintaining specificity. Further large-scale studies specifically exploring the comparison between high b-value bpMRI and mpMRI should be made to acquire an exact result.

There are several potential limitations in our review. First, the included studies were heterogeneous in their methods, which affected the general applicability of the

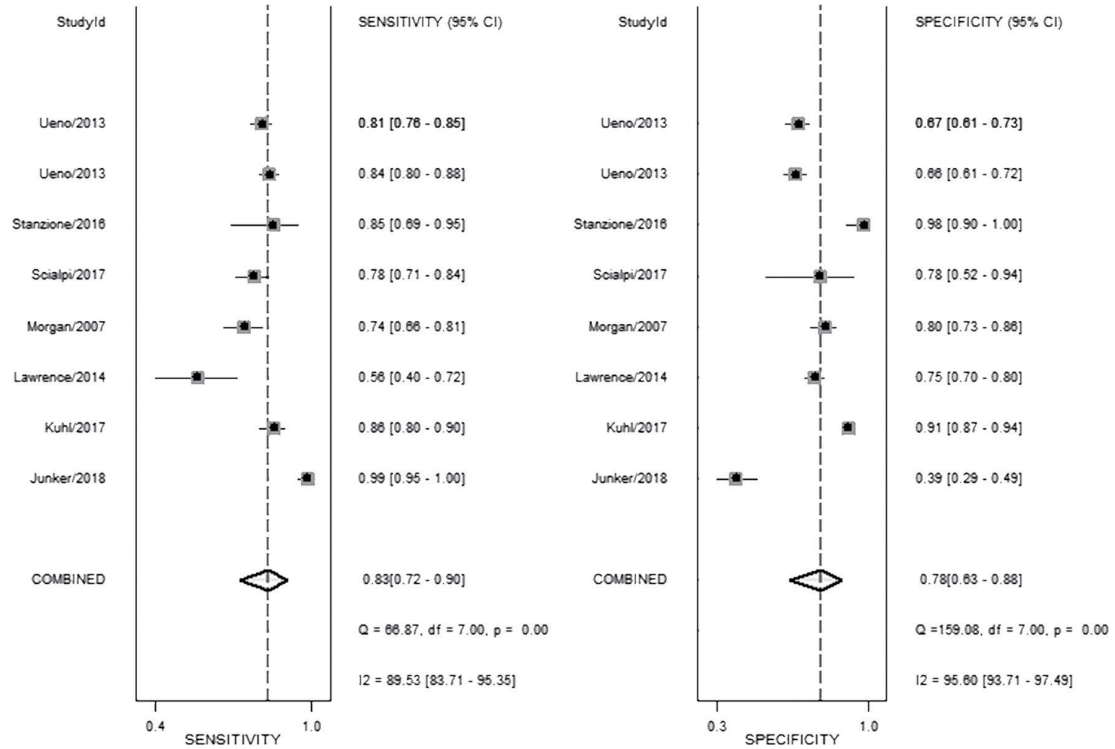

Figure 13 Coupled forest plots show pooled estimates of sensitivity and specificity of biparametric MRI combined with high b value MRI.

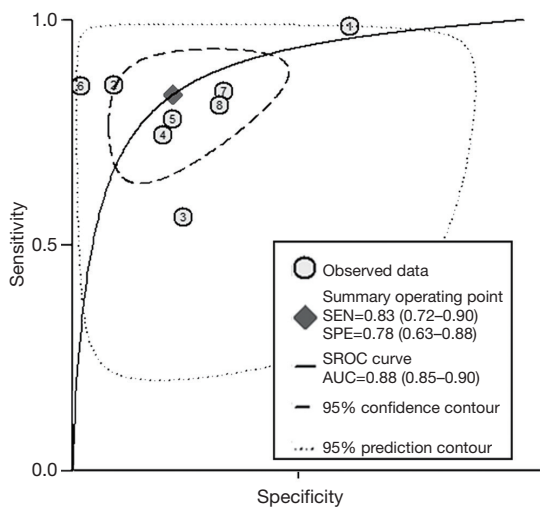

Figure 14 Summary ROC (SROC) curves with prediction and confidence contours of biparametric MRI combined with high b value MRI

summary estimates. To explore the heterogeneity of our data, we performed meta-regression and multiple subgroup analysis so that the diagnostic accuracy of bpMRI could be improved in the future. Second, until recently the definition of clinically relevant PCa varied considerably between each studies, which might have resulted in unreliable conclusions in our study. Third, studies with negative results are less likely to be published, which may lead to exaggeration of the beneficial effects in meta-analysis. Fourth, the different versions of PI-RADS score the included studies used may have an impact on our results. Finally, our meta-analysis focused on newly diagnosed or clinically suspected PCa. The results of our meta-analysis do not apply to detection or staging of recurrent PCa.

Conclusions

A head-to-head comparison showed that the performance of bpMRI was similar to that of mpMRI for the diagnosis of PCa though the sensitivity was significantly lower. With the combination of high b value MRI, the sensitivity and specificity could improve to 0.83 and 0.78 respectively. The result of multiple subgroup analysis showed consistency with overall pooled estimates.

Acknowledgments

Funding: None.

Footnote

Conflicts of Interest: All authors have completed the ICMJE uniform disclosure form (available at http://dx.doi.org/10.21037/tau.2020.02.03). The authors have no conflicts of interest to declare.

Ethical Statement: The authors are accountable for all aspects of the work in ensuring that questions related to the accuracy or integrity of any part of the work are appropriately investigated and resolved.

References

1. Todua F, Gagua R, Maglakelidze M, et al. Cancer incidence and mortality - Major patterns in GLOBOCAN 2012, worldwide and Georgia, 2015. Available online: http://science.org.ge/old/moambe/9-1/Todua%20Fridon.
2. Haas GP, Delongchamps N, Brawley OW, et al. The worldwide epidemiology of prostate cancer: perspectives from autopsy studies. Can J Urol 2008;15:3866-71.
3. Weinreb JC, Barentsz JO, Choyke PL, et al. PI-RADS Prostate Imaging - Reporting and Data System: 2015, Version 2. Eur Urol 2016;69:16-40.
4. Johnson LM, Turkbey B, Figg WD, et al. Multiparametric MRI in prostate cancer management. Nat Rev Clin Oncol 2014;11:346-53.
5. Barentsz JO, Richenberg J, Clements R, et al. ESUR prostate MR guidelines 2012. Eur Radiol 2012;22:746-57.
6. Woo S, Suh CH, Kim SY, et al. Head-to-Head Comparison Between Biparametric and Multiparametric MRI for the Diagnosis of Prostate Cancer: A Systematic Review and Meta-Analysis. AJR Am J Roentgenol 2018;211:W226-41.
7. Kuhl CK, Bruhn R, Kramer N, et al. Abbreviated Biparametric Prostate MR Imaging in Men with Elevated Prostate-specific Antigen. Radiology 2017;285:493-505.
8. Boesen L, Norgaard N, Logager V, et al. Assessment of the Diagnostic Accuracy of Biparametric Magnetic Resonance Imaging for Prostate Cancer in Biopsy-Naive Men: The Biparametric MRI for Detection of Prostate Cancer (BIDOC) Study. JAMA Netw Open 2018;1:e180219.
9. Greer MD, Shih JH, Lay N, et al. Validation of the Dominant Sequence Paradigm and Role of Dynamic Contrast-enhanced Imaging in PI-RADS Version 2. Radiology 2017;285:859-69.
10. Puech P, Randazzo M, Ouzzane A, et al. How are we going to train a generation of radiologists (and urologists) to read prostate MRI? Curr Opin Urol 2015;25:522-35.
11. Vargas HA, Akin O, Franiel T, et al. Diffusion-weighted endorectal MR imaging at 3 T for prostate cancer: tumor detection and assessment of aggressiveness. Radiology 2011;259:775-84.
12. Aydin H, Hekimogl B, Tatar IG. Limitations, disabilities, and pitfalls of dynamic contrast-enhanced MRI as a diagnostic modality in prostate cancer. AJR Am J Roentgenol 2013;200:W326.
13. Berman RM, Brown AM, Chang SD, et al. DCE MRI of prostate cancer. Abdom Radiol (NY) 2016;41:844-53.
14. Ganeles J, Zollner A, Jackowski J, et al. Immediate and early loading of Straumann implants with a chemically modified surface (SLActive) in the posterior mandible and maxilla: 1-year results from a prospective multicenter study. Clin Oral Implants Res 2008;19:1119-28.
15. Wallace B, J Dahabreh I, Trikalinos T, et al. Closing the Gap between Methodologists and End-Users: R as a Computational Back-End. J Stat Softw 2011;49:1-15.
16. Reitsma JB, Glas AS, Rutjes AW, et al. Bivariate analysis of sensitivity and specificity produces informative summary measures in diagnostic reviews. J Clin Epidemiol 2005;58:982-90.
17. Higgins JP, Thompson SG, Deeks JJ, et al. Measuring inconsistency in meta-analyses. BMJ 2003;327:557-60.
18. Afifi A, Ali Ramadan A, Alabbady A, et al. Multi-parametric MRI and PI-RADS (V1) scoring system: New inception in cancer prostate diagnosis to evaluate diagnostic performance of different score combinations. Egypt J Radiol Nucl Med 2016;47:1083-94.
19. Agha M, Eid A. 3 Tesla MRI surface coil: Is it sensitive for prostatic imaging. 2014. Available online: https://pdf.sciencedirectassets.com

20. Barth BK, De Visschere PJL, Cornelius A, et al. Detection of Clinically Significant Prostate Cancer: Short Dual-Pulse Sequence versus Standard Multiparametric MR Imaging-A Multireader Study. Radiology 2017;284:725-36.
21. Brock M, Roghmann F, Sonntag C, et al. Fusion of Magnetic Resonance Imaging and Real-Time Elastography to Visualize Prostate Cancer: A Prospective Analysis using Whole Mount Sections after Radical Prostatectomy. Ultraschall Med 2015;36:355-61.
22. Delongchamps NB, Beuvon F, Eiss D, et al. Multiparametric MRI is helpful to predict tumor focality, stage, and size in patients diagnosed with unilateral low-risk prostate cancer. Prostate Cancer Prostatic Dis 2011;14:232-7.
23. Delongchamps NB, Rouanne M, Flam T, et al. Multiparametric magnetic resonance imaging for the detection and localization of prostate cancer: combination of T2-weighted, dynamic contrast-enhanced and diffusion-weighted imaging. BJU Int 2011;107:1411-8.
24. Franiel T, Stephan C, Erbersdobler A, et al. Areas suspicious for prostate cancer: MR-guided biopsy in patients with at least one transrectal US-guided biopsy with a negative finding--multiparametric MR imaging for detection and biopsy planning. Radiology 2011;259:162-72.
25. Haider MA, van der Kwast TH, Tanguay J, et al. Combined T2-Weighted and Diffusion-Weighted MRI for Localization of Prostate Cancer. AJR Am J Roentgenol 2007;189:323-8.
26. Isebaert S, Van den Bergh L, Haustermans K, et al. Multiparametric MRI for prostate cancer localization in correlation to whole-mount histopathology. J Magn Reson Imaging 2013;37:1392-401.
27. Jambor I, Kahkonen E, Taimen P, et al. Prebiopsy multiparametric 3T prostate MRI in patients with elevated PSA, normal digital rectal examination, and no previous biopsy. J Magn Reson Imaging 2015;41:1394-404.
28. Kitamura K, Muto S, Yokota I, et al. Feasibility of multiparametric prostate magnetic resonance imaging in the detection of cancer distribution: histopathological correlation with prostatectomy specimens. Prostate Int 2014;2:188-95.
29. Lee DH, Nam JK, Lee SS, et al. Comparison of Multiparametric and Biparametric MRI in First Round Cognitive Targeted Prostate Biopsy in Patients with PSA Levels under 10 ng/mL. Yonsei Med J 2017;58:994-9.
30. Morgan VA, Kyriazi S, Ashley SE, et al. Evaluation of the potential of diffusion-weighted imaging in prostate cancer detection. Acta Radiol 2007;48:695-703.
31. Rinaldi D, Fiocchi F, Ligabue G, et al. Role of diffusion-weighted magnetic resonance imaging in prostate cancer evaluation. Radiol Med 2012;117:1429-40.
32. Rais-Bahrami S, Siddiqui MM, Vourganti S, et al. Diagnostic value of biparametric magnetic resonance imaging (MRI) as an adjunct to prostate-specific antigen (PSA)-based detection of prostate cancer in men without prior biopsies. BJU Int 2015;115:381-8.
33. Baur AD, Maxeiner A, Franiel T, et al. Evaluation of the prostate imaging reporting and data system for the detection of prostate cancer by the results of targeted biopsy of the prostate. Invest Radiol 2014;49:411-20.
34. Doo KW, Sung DJ, Park BJ, et al. Detectability of low and intermediate or high risk prostate cancer with combined T2-weighted and diffusion-weighted MRI. Eur Radiol 2012;22:1812-9.
35. Fascelli M, Rais-Bahrami S, Sankineni S, et al. Combined Biparametric Prostate Magnetic Resonance Imaging and Prostate-specific Antigen in the Detection of Prostate Cancer: A Validation Study in a Biopsy-naive Patient Population. Urology 2016;88:125-34.
36. Iwazawa J, Mitani T, Sassa S, et al. Prostate cancer detection with MRI: is dynamic contrast-enhanced imaging necessary in addition to diffusion-weighted imaging? Diagn Interv Radiol 2011;17:243-8.
37. Jung SI, Donati OF, Vargas HA, et al. Transition Zone Prostate Cancer: Incremental Value of Diffusion-weighted Endorectal MR Imaging in Tumor Detection and Assessment of Aggressiveness. Radiology 2013;269:493-503.
38. Junker D, Steinkohl F, Fritz V, et al. Comparison of multiparametric and biparametric MRI of the prostate: are gadolinium-based contrast agents needed for routine examinations? World J Urol 2019;37:691-9.
39. Katahira K, Takahara T, Kwee TC, et al. Ultra-high-b-value diffusion-weighted MR imaging for the detection of prostate cancer: evaluation in 201 cases with histopathological correlation. Eur Radiol 2011;21:188-96.
40. Kitajima K, Kaji Y, Fukabori Y, et al. Prostate cancer detection with 3 T MRI: comparison of diffusion-weighted imaging and dynamic contrast-enhanced MRI in combination with T2-weighted imaging. J Magn Reson Imaging 2010;31:625-31.
41. Lawrence EM, Tang SY, Barrett T, et al. Prostate cancer: performance characteristics of combined T(2)W and DW-MRI scoring in the setting of template transperineal re-biopsy using MR-TRUS fusion. Eur Radiol 2014;24:1497-505.
42. Lim HK, Kim JK, Kim KA, et al. Prostate cancer: apparent diffusion coefficient map with T2-weighted images for

detection--a multireader study. Radiology 2009;250:145-51.
43. Mussi TC, Martins T, Garcia RG, et al. Are Dynamic Contrast-Enhanced Images Necessary for Prostate Cancer Detection on Multiparametric Magnetic Resonance Imaging? Clin Genitourin Cancer 2017;15:e447-54.
44. Naiki T, Okamura T, Nagata D, et al. Preoperative prediction of neurovascular bundle involvement of localized prostate cancer by combined T2 and diffusion-weighted imaging of magnetic resonance imaging, number of positive biopsy cores, and Gleason score. Asian Pac J Cancer Prev 2011;12:909-13.
45. Rosenkrantz AB, Mannelli L, Kong X, et al. Prostate cancer: utility of fusion of T2-weighted and high b-value diffusion-weighted images for peripheral zone tumor detection and localization. J Magn Reson Imaging 2011;34:95-100.
46. Scialpi M, Prosperi E, D'Andrea A, et al. Biparametric versus Multiparametric MRI with Non-endorectal Coil at 3T in the Detection and Localization of Prostate Cancer. Anticancer Res 2017;37:1263-71.
47. Schimmöller L, Quentin M, Arsov C, et al. MR-sequences for prostate cancer diagnostics: validation based on the PI-RADS scoring system and targeted MR-guided in-bore biopsy. Eur Radiol 2014;24:2582-9.
48. Shimofusa R, Fujimoto H, Akamata H, et al. Diffusion-weighted imaging of prostate cancer. J Comput Assist Tomogr 2005;29:149-53.
49. Stanzione A, Imbriaco M, Cocozza S, et al. Biparametric 3T Magnetic Resonance Imaging for prostatic cancer detection in a biopsy-naive patient population: a further improvement of PI-RADS v2? Eur J Radiol 2016;85:2269-74.
50. Tamada T, Sone T, Higashi H, et al. Prostate cancer detection in patients with total serum prostate-specific antigen levels of 4-10 ng/mL: diagnostic efficacy of diffusion-weighted imaging, dynamic contrast-enhanced MRI, and T2-weighted imaging. AJR Am J Roentgenol 2011;197:664-70.
51. Tanimoto A, Nakashima J, Kohno H, et al. Prostate cancer screening: The clinical value of diffusion-weighted imaging and dynamic MR imaging in combination with T2-weighted imaging. J Magn Reson Imaging 2007;25:146-52.
52. Thestrup KC, Logager V, Baslev I, et al. Biparametric versus multiparametric MRI in the diagnosis of prostate cancer. Acta Radiol Open 2016;5:2058460116663046.
53. Ueno Y, Kitajima K, Sugimura K, et al. Ultra-high b-value diffusion-weighted MRI for the detection of prostate cancer with 3-T MRI. J Magn Reson Imaging 2013;38:154-60.
54. Ueno Y, Takahashi S, Kitajima K, et al. Computed diffusion-weighted imaging using 3-T magnetic resonance imaging for prostate cancer diagnosis. Eur Radiol 2013;23:3509-16.
55. Vilanova JC, Barcelo-Vidal C, Comet J, et al. Usefulness of prebiopsy multifunctional and morphologic MRI combined with free-to-total prostate-specific antigen ratio in the detection of prostate cancer. AJR Am J Roentgenol 2011;196:W715-22.
56. De Visschere P, Lumen N, Ost P, et al. Dynamic contrast-enhanced imaging has limited added value over T2-weighted imaging and diffusion-weighted imaging when using PI-RADSv2 for diagnosis of clinically significant prostate cancer in patients with elevated PSA. Clin Radiol 2017;72:23-32.
57. Yağci AB, Ozari N, Aybek Z, et al. The value of diffusion-weighted MRI for prostate cancer detection and localization. Diagn Interv Radiol 2011;17:130-4.
58. Yoshimitsu K, Kiyoshima K, Irie H, et al. Usefulness of apparent diffusion coefficient map in diagnosing prostate carcinoma: correlation with stepwise histopathology. J Magn Reson Imaging 2008;27:132-9.
59. Yoshizako T, Wada A, Hayashi T, et al. Usefulness of Diffusion-Weighted Imaging and Dynamic Contrast-Enhanced Magnetic Resonance Imaging in the Diagnosis of Prostate Transition-Zone Cancer. Acta Radiol 2008;49:1207-13.
60. Boesen L, Norgaard N, Logager V, et al. Prebiopsy Biparametric Magnetic Resonance Imaging Combined with Prostate-specific Antigen Density in Detecting and Ruling out Gleason 7-10 Prostate Cancer in Biopsy-naive Men. Eur Urol Oncol 2019;2:311-9.
61. Knaapila J, Jambor I, Perez IM, et al. Prebiopsy IMPROD Biparametric Magnetic Resonance Imaging Combined with Prostate-Specific Antigen Density in the Diagnosis of Prostate Cancer: An External Validation Study. Eur Urol Oncol 2019. [Epub ahead of print].
62. Gayet M, van der Aa A, Beerlage HP, et al. The value of magnetic resonance imaging and ultrasonography (MRI/US)-fusion biopsy platforms in prostate cancer detection: a systematic review. BJU Int 2016;117:392-400.
63. Niu XK, Chen XH, Chen ZF, et al. Diagnostic Performance of Biparametric MRI for Detection of Prostate Cancer: A Systematic Review and Meta-Analysis. AJR Am J Roentgenol 2018;211:369-78.
64. Hara N, Okuizumi M, Koike H, et al. Dynamic contrast-enhanced magnetic resonance imaging (DCE-MRI) is a useful modality for the precise detection and staging of

early prostate cancer. Prostate 2005;62:140-7.
65. Kozlowski P, Chang SD, Jones EC, et al. Combined diffusion-weighted and dynamic contrast-enhanced MRI for prostate cancer diagnosis--correlation with biopsy and histopathology. J Magn Reson Imaging 2006;24:108-13.
66. Franiel T, Ludemann L, Rudolph B, et al. Evaluation of normal prostate tissue, chronic prostatitis, and prostate cancer by quantitative perfusion analysis using a dynamic contrast-enhanced inversion-prepared dual-contrast gradient echo sequence. Invest Radiol 2008;43:481-7.
67. Maas MC, Futterer JJ, Scheenen TW. Quantitative evaluation of computed high B value diffusion-weighted magnetic resonance imaging of the prostate. Invest Radiol 2013;48:779-86.
68. Syer TJ, Godley KC, Cameron D, et al. The diagnostic accuracy of high b-value diffusion- and T2-weighted imaging for the detection of prostate cancer: a meta-analysis. Abdom Radiol (NY) 2018;43:1787-97.

Cite this article as: Liang Z, Hu R, Yang Y, An N, Duo X, Liu Z, Shi S, Liu X. Is dynamic contrast enhancement still necessary in multiparametric magnetic resonance for diagnosis of prostate cancer: a systematic review and meta-analysis. Transl Androl Urol 2020;9(2):553-573. doi: 10.21037/tau.2020.02.03

